Nonlinear Dynamics of Brake Squeal

by: M. L. Chargin[1], L. W. Dunne[2], and D. N. Herting[2]

Abstract

An efficient procedure for the analysis of brake squeal using MSC/NASTRAN models is described. A unique nonlinear method accounts for both superelement modes and surface friction data. The motions at the pad/rotor interface are described by small velocities and pressures relative to the steady-state condition. Both Transient Analysis and Complex Eigenvalues are provided analysis of brake systems.

1.0 INTRODUCTION

This paper describes the development of the BSQL computer program by CDH GmbH designed to simulate high-frequency nonlinear dynamics. This code is an analytic postprocessor for MSC/NASTRAN designed primarily for numerical simulation of the phenomenon known as disk brake squeal. This document contains a description of the theory and capabilities of the system along with results for small brake models.

Brake squeal is generally defined as an unpleasant, self-induced, high frequency (2000 to 10000 Hz), vibration that occurs on disk brakes. Until recently the only information on the physics of brake squeal was obtained by physical tests. Experiments from the literature revealed that the displacements resembled the mode shapes of the stationary systems and the frequency of squeal was similar to the natural frequencies of the corresponding rotor mode. However, the temperature, pressure, and damping also effected the results. Changing the friction properties of the brake pads had a major effect on the onset (or lack of) squeal.

It is significant that in experiments the frequency spectrum of the squeal indicates that the peaks occur at even multiples of the fundamental frequency. Since the normal mode frequencies do not follow this pattern, one deducts that nonlinear behavior is causing a non-sinusoidal response.

---

[1] NASA Ames Research Center

[2] CDH GmbH, Ingolstadt Germany

Early attempts at an analytic approach used simple lumped parameter models used only one or two modes to demonstrate divergence. The Unsymmetric friction effects in the equations of motion may cause a non-conservative system which potentially can diverge. However, these models could not predict actual hardware behavior where many modes and nonlinear friction effects are present. The next stage was to expand these systems using more accurate finite element models.

In the current approach the fundamental physics of the brake squeal problem are simulated by a step-by-step transient integration of the equations of motion to account for the high frequency nonlinear dynamics. The basic structure is represented by matrices and loads produced by an MSC/NASTRAN finite element model. All structural components may be modeled with precise detail, and may include sliding joints and other linear contact. However, the nonlinear analysis procedure is optimized in the BSQL program specifically for the brake pad and rotor friction effects.

To provide further insight into the physical aspects of a particular state of the system, the tangent matrices (e.g.. Jacobian) may be captured at the steady-state initial condition or at any point in the transient solution. These matrices may be transferred to a Complex Eigenvalue analysis in MSC/NASTRAN to identify the critical mode shapes and damping factors. This form of data output is more convenient and will allow easier visualization of the motions.

2.0 THEORETICAL APPROACH

The basic theory for disk brake squeal analysis assumes that the stationary “pads” are in full contact with a rotating disk “rotor”. The friction force that develops on each small area will be a general function of the local pressure, velocity, and temperature. The rotational inertia effects of the rotor are assumed to be negligible at the high frequencies of the squeal vibrations. Additional physical effects such as the properties of the dust have been considered but are not discussed here.

A linear finite element model of the pad, rotor, caliper and surrounding structure will be represented by its reduced matrices. Typically a fine mesh model can be reduced to the contact points and modal coordinates using component modal synthesis methods in MSC/NASTRAN. The reduced matrices will include the physical properties of the piston, fluid, rubber seals, and all important flexible modes.

Nonlinear Friction Forces

The surface laws for contact and friction will be performed on individual pairs of pad and rotor grid points. At each time step or iteration and for each pair "p" and "r" the following information is available

- $\{S_p\}$ - the area vector (outward) on the pad point.
- V_y - the steady circumferential velocity of the rotor at the point.
- $\{v_p\}$ - the 3 velocities of the pad point from the current solution vector
- $\{v_r\}$ - the 3 velocities of the rotor point, relative to V_y.
- F_z - the incremental normal force at the point, based upon the structural motions.

At each iteration the following equations are used for each "gap" element: The normal pressure, p_n is:

$$p_n = F_z / |\{S_p\}| + P_o \tag{1}$$

where P_o is a user supplied preload on the system. All displacements, stresses, and load outputs will be measured relative to this initial state.

The relative velocity vector, $\{\Delta v\}$, between the pad and rotor, is:

$$\{\Delta v\} = \{v_r\} - \{v_p\} + \{0, V_y, 0\} \tag{2}$$

The tangent velocity vector is obtained by subtracting the normal component

$$\{V_t\} = \{\Delta v\} - (\{\Delta v\} \cdot \{n\})\{n\} \tag{3}$$

The friction force is obtained with an interpolation scheme using tabular inputs:

$$F_t = \mu(p_n, |\{V_t\}|, T) * A * p_n \tag{4}$$

The tangent force F_t is converted to force vectors on the pad and rotor and added to the global force vector. The direction of the force will depend upon the velocity.

A special procedure avoids numerical problems at very small velocities. If $(|\{V_t\}| < 10 * V_{TOL})$ where V_{TOL} is user-defined, then to avoid discontinuities, an arctangent function will be used to modify the forces in the transition zone. Symbolically:

$$F_t = F_t * (2/\pi) * \arctan\left(\left| \{V_t\} \right| / V_{TOL} \right) \tag{5}$$

For all cases:

$$\{F_p\} = \{F_p\} + F_t * \{V_t\} / \left| \{V_t\} \right| \quad \text{(Forces on pad)} \tag{6}$$

and:
$$\{F_r\} = \{F_r\} - F_t * \{V_t\} / \left| \{V_t\} \right| \quad \text{(Forces on rotor)} \tag{7}$$

Note that we are assuming that the normal forces are linear and the pad and rotor points remain in contact.

System Integration

The Brake Squeal simulation is performed with a step-by-step integration of the nonlinear dynamics in the time domain. A higher order implicit transient integration algorithm is used for its advantages over explicit methods for the particular problems with large, highly coupled, constrained equations. The full theory is given in Ref. 4. The theoretical interfaces for BSQL are defined below.

The matrix equation for equilibrium at any time step is:

$$[M]\{\ddot{u}\} + [B]\{\dot{u}\} + [K]\{u\} = \{P(t)\} + \{Q\} + \{F_f(\lambda, \dot{u})\} \tag{8}$$

Where:

$[M]$, $[B]$, $[K]$, and $\{P(t)\}$ are linear FE matrices and loads.

$\{Q\}$ are the Forces of Constraint resulting from pad/rotor contact.

$\{F_f(\lambda, \dot{u})\}$ are the nonlinear friction forces resulting from pad/rotor sliding..

At this point introduce a constraint equation between the normal displacements of the disk and the pad. At each contact point:

$$\left(\vec{u}_d - \vec{u}_p \right) \bullet \vec{n} = 0 \tag{9}$$

This equation implies that the pad and disk are in contact at all times during the solution of the problem. Note that if the initial conditions are satisfied, the first or second time derivatives of $\{u\}$ may be used. For reasons of numerical stability, differentiate the above constraint twice to obtain:

$$\begin{aligned} v &= \dot{u} \\ \dot{v} &= \ddot{u} \end{aligned} \tag{10}$$

and

$$\left(\vec{v}_d - \vec{v}_p\right) \bullet n = 0 \text{ or } [G]\{\vec{v}\} = 0 \tag{11}$$

In order to implement the constraints we define Lagrange multipliers which provide the following matrix relationship for the forces:

$$\{Q\} = -[G]^T \{\dot{\lambda}\} \tag{12}$$

Each Lagrange multiplier, $\dot{\lambda}$, represents the total contact force on a pad point.

In order to solve the above system in the DASSL transient solver, the equations must be combined into a single first order differential equation of the form:

$$\{f(t, y, \dot{y})\} = \{0\} \tag{13}$$

In order to solve the equations, the $\{y\}$ and $\{f\}$ vectors contain three partitions of the form:

$$\{y\} = \begin{Bmatrix} v \\ \lambda \\ u \end{Bmatrix} \tag{14}$$

where $$\{v\} = \{\dot{u}\} \tag{15}$$

Corresponding to Eq.'s (8),(12), and (10), the respective partitions of the generalized force, $\{f\}$, corresponding to the vector, $\{y\}$, are:

$$\{f\} = \begin{Bmatrix} F_v \\ F_\lambda \\ F_u \end{Bmatrix} = \begin{Bmatrix} M\dot{v} + Bv + Ku + G^T\lambda - P(t) - F_f(\lambda, \dot{u}) \\ \hline G\dot{v} \\ \hline -v + \dot{u} \end{Bmatrix} \tag{16}$$

The nonlinear terms in Eq. (16) are generated by the gap element friction forces at each iteration. The right hand vector is evaluated at every trial state of the solution using the gap forces and simple multiplication. At each time step the program iterates until the F_y vectors in Eq. (16) are less than an error tolerance. Note: In the actual solution the third partition is not an active part of the solution, but is shown for consistency.

Another required interface with the DASSL Transient Solver are the tangent matrices which are defined as $[\partial f/\partial y]$ and $[\partial f/\partial \dot{y}]$. These are obtained by taking

the partial derivatives of Eq. 16. A major part of the process is the matrix solution of the Jacobian which is defined as

$$[J] = \left[\frac{\partial f}{\partial y}\right] + \alpha\left[\frac{\partial f}{\partial \dot{y}}\right] \tag{17}$$

Where α is an integration operator. Using Eqs. (16) and (17), the Jacobian can be written as

$$[J] = \left[\begin{array}{c|c|c} \alpha M + B & \alpha H^T & K + \alpha C_f \\ \hline \alpha G & 0 & 0 \\ \hline -I & 0 & \alpha I \end{array}\right] \tag{18}$$

where $[H]^T = [G]^T + \left[\partial F_f / \partial \dot{\lambda}\right]$ and $[C_f] = [\partial F_f / \partial v]$. Since the $[C_f]$ damping matrix partition could become large, it will be included only for the complex Eigenvalue solution.

Only the tangent partitions of $\{F_f\}$ are calculated at each surface friction point when the solution routine requests an update of the Jacobian matrix. All other matrix terms will remain constant over the time of the solution.

The matrices need to be formed and decomposed only when the convergence becomes slow or the time step size is changed. The constant matrices may be precalculated once at the beginning of the job resulting in a large cost saving. Details of the actual numerical implementation of the transient solver, DASSL, are given in Reference 4.

Solution Steps

An advantage of the CDH analysis system is that it will simulate the more important physics of the brake dynamics with a minimum of a-priori assumptions. Namely:

- Realistic simulations will be assured by allowing the use of detailed models to represent higher eigenfrequencies.
- Efficient nonlinear solutions are obtained by using a reduced modal representation.
- Design changes may be quickly evaluated by the use of superelements in the linear model
- A general friction law is provided for the pad/rotor interface, allowing empirical tables obtained from actual experiments.

The simulation requires four steps, as shown in Fig. 1, and described below.

1. The linear portion of the problem is modeled in MSC/NASTRAN. However, other popular FE codes which have the capability of providing reduced output matrices in ASCII format may be adapted with some manual conversion effort. The model may include as much of the caliper, hub, rotor, piston(s), and suspension structure as necessary.
2. The basic conversion of the MSC/NASTRAN data is controlled by the PREBSQL code. It requires simple parameter inputs and the NASTRAN geometry tables and reduced matrices to produce the contact element data for the pad/rotor interface. Any number of contact surfaces is allowed.
3. BSQL will process the surface contact information such as friction and pressure loads and couple these loads to the structure at each time step. The complete dynamic motions are integrated over a period of time defined by the user. The objective is to produce accurate time history tables and plotting information.
4. The PLOTIT program supplied with the system will extract selected records of time history for points and GAP elements. Displacements, velocities, accelerations, contact forces, and total friction coefficients may be recovered.

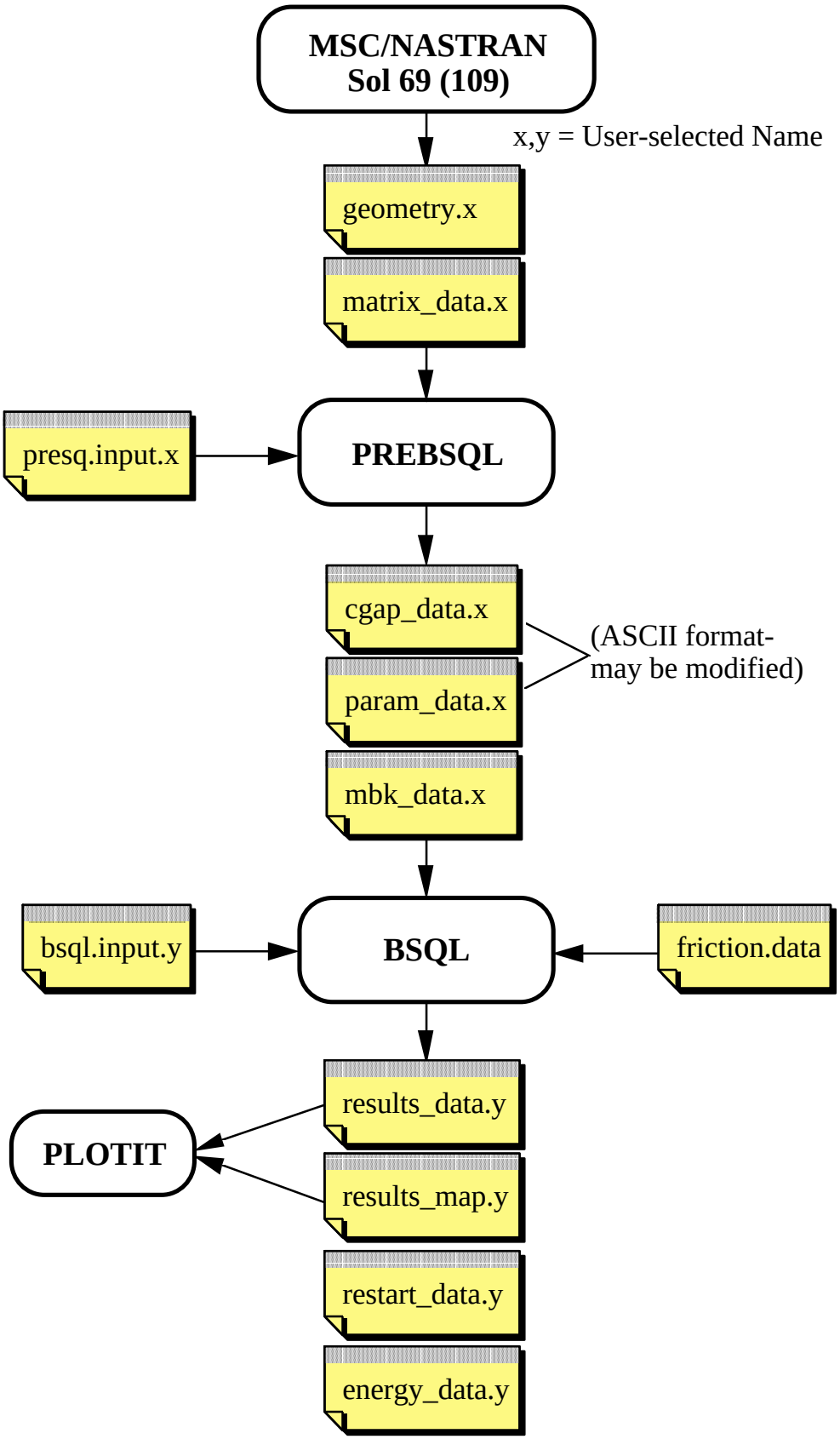

Figure 1, Execution steps in Brake Squeal Analysis

The BSQL output consists of three tabular response data files and a restart file. The restart file is available to start the BSQL process at a specific point in time with changes in the parameter inputs. The response files consist of a binary database of time histories for the selected output points and a map table which identifies the locations of the data for each response point. The PLOTIT program will format the output time steps and selected outputs into an ASCII table similar to a spreadsheet. The third tabular ASCII file "energy.y" contains various energy measures as a function of time.

User Inputs

In summary the user must supply the following input data for the complete analysis:

1. A finite element model of the disk brake system with enough detail of the caliper and pads to represent frequencies of 10000 Hz. (corresponding to wavelengths of ~500 mm. in steel). The FE model should include the sliding parts, such as the piston and other mechanisms.
2. Two sets of loads must be supplied with the FE model. The first load is a unit pressure on the inner contact surfaces of the pads. The second load defines a force on the actuator piston corresponding to a selected force on the brake pedal.
3. The pad-rotor interface should consist of grid points on both surfaces having nearly-identical locations at the start of contact. The PREBSQL program will find these points and generate internal "GAP" elements which are used to calculate the contact and friction forces.
4. The input pad-rotor friction law may be provided either by a simple equation or by multiple tables. The coefficient of friction is specified as a function of velocity, normal force, and temperature.
5. Miscellaneous constants such as rotor velocity, pad damping, time step size, and pedal forces are supplied as parameters on the input file to the BSQL program.

6. Solution controls in BSQL are available to specify the amount of retained output data, select convergence tolerances, and save data for restarts.

Complex Eigenvalue Analysis

Although the nonlinear transient solution from BSQL provides accurate simulations of the model's dynamics, it also provides an overwhelming amount of data. The complex Eigenvalue analysis can provide some insight to the physical dynamic effects of a diverging or nearly-diverging system from a smaller amount of output data. In effect this analysis may be used to examine small motions about a nonlinear steady-state condition.

In this approach the BSQL code will generate the tangent matrix partitions related to contact and friction as described in Eq. 18. These matrices will depend upon the contact forces and the local sliding velocities. They may be obtained from a steady-state analysis as used in the initialization process or from a selected point in the analysis. Solution 107 of MSC/NASTRAN has been modified to read the BSQL matrices and assemble the solution matrices for a particular combination of pressure, velocity, and temperature.

The complex Eigenvalue equation in MSC/NASTRAN is:

$$\left(p^2[M_{dd}] + p[B_{dd}] + [K_{dd}]\right)\{\psi\} = 0 \tag{19}$$

The corresponding terms from BSQL are:

$$\{\psi\} = \begin{Bmatrix} u \\ \lambda \end{Bmatrix} \tag{20}$$

$$\{v\} = p\{\psi\} \tag{21}$$

$$[M_{dd}] = \begin{bmatrix} M & H^T \\ G & 0 \end{bmatrix} \tag{22}$$

$$[B_{dd}] = \begin{bmatrix} B + C_f & 0 \\ 0 & 0 \end{bmatrix} \tag{23}$$

$$[K_{dd}] = \begin{bmatrix} K & 0 \\ 0 & 0 \end{bmatrix} \tag{24}$$

Note that the matrix [K] may also contain damping terms that are available in this solution such as the parameter G and the material structural damping inputs.

The problem with this formulation is that the current Lanczos algorithm in MSC/NASTRAN attempts to extract a zero-frequency root for every λ degree of freedom. This creates a high cost and a large output file. Other alternatives are being tested currently.

The major drawback to the complex Eigenvalue approach is that it requires a nonlinear solution with friction effects to obtain the correct tangent matrices. This solution sequence will also ignore all nonlinear effects such as limit cycles. (This may create some uncertainty as to the magnitude of some unstable modes.) However, once an unstable condition at a particular state is determined from the transient analysis, the overall physical response can be examined more conveniently by plotting the eigenvectors of the unstable complex modes.

3.0 SAMPLE DISK BRAKE PROBLEM

A very simple disk brake model was developed to test the various code options and to verify the results. There is no theoretical solution for this problem, but by changing the friction characteristics and other parameters, one can observe the differences in the brake squeal behavior. The model has been used for previous studies and is not proprietary.

The finite element model of the complete structure is shown in Fig. 2 The pads are modeled with only one HEXA element, so it clearly is a simplistic model. In this case the pads and the rotor have coincident grid points in the contact area.

The rotor, caliper, and pads are all defined as separate superelements, in order to simulate the process for the real brake analysis. The MSC/NASTRAN input deck is listed at the end of this section. Following the MSC/NASTRAN execution, one must execute the PREBSQL program.

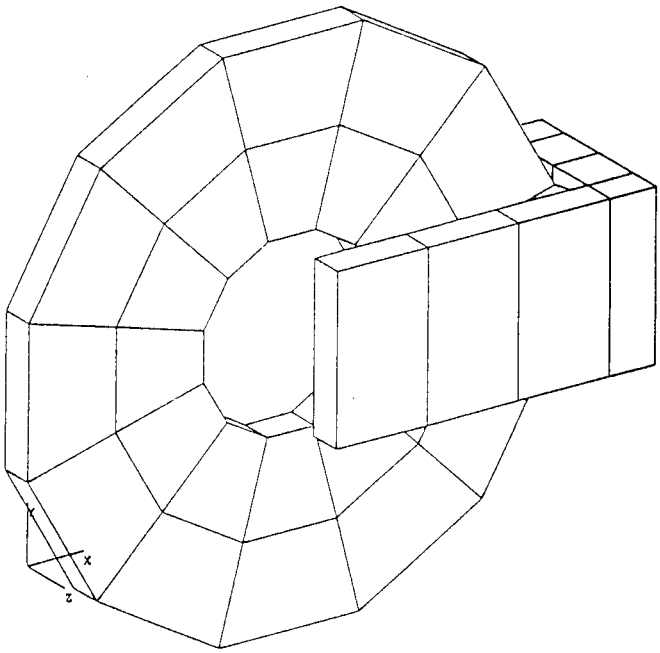

Fig. 2 Sample disk brake model

Following the completion of PREBSQL, BSQL code was executed numerous times to test the various combinations of key parameters. This problem was used as a test bed to evaluate the effects of different parameters, as well as establishing the default parameter values. A typical input to the BSQL program is:

```
$-----------------------------------------------------------------------
$ RPM
  143.239
$ PARAM, G,  W3, and W4
       0.0, 0.0, 0.0
$ PMAX and TLOAD
  1.0,     0.0005
$ VTOL
  0.001
$ TFINAL, ATOL1  , ATOL2  , RTOL1   , RTOL2 , MAXORD  , TOLINT
  0.006 , 0.0001 , 1.E+20 , 0.00001 , 0.0   , 2       , 1.E-10
$
$ NRSTRT, NOUTPT, RESTART
    1000,      2, 0
$-----------------------------------------------------------------------
$ Specify specific Grid Temperatures
$-----------------------------------------------------------------------
$ No grid temperatures for this case
$
$-----------------------------------------------------------------------
```

$----------
OUTPUT
107, 324, 111, 321, 99005

The key parameters are shown in **bold** letters. For all cases, the following parameters had a fixed value.

- RPM was set to 143.239. (Corresponding to 15 rad/sec)
- Absolute tolerance for the disp., and velo., ATOL1, was set to 0.0001.
- The absolute tolerance for the Lagrange Multipliers, ATOL2, was set to 1.E+20, which means that absolute tolerance measure is not used.
- The relative tolerance for the Lagrange Multipliers, RTOL2, was set to 0.0, which again, ignores its effect.
- The maximum order of integration was set to 2.
- The convergence tolerance for the initial conditions was set to 1.E-10.

The three most interesting parameters that were studied are:

a) error ratio tolerance limit for the disp., velo., and acce., RTOL1
b) the value of the friction coefficient, μ
c) the time required for the applied load to reach its peak, TLOAD

The following table lists the characteristics of the computations that were performed in the study.

Case	RTOL1	TLOAD	μ	G	W3	P0	TF	NS	CPU
1	.00001	.0005	0.7-.0005V	0.	0.	40.	0.006	2504	15.0
2	.0001	.0005	0.7-.0005V	0.	0.	40.	0.006	2300	14.1
3	.0001	.0005	0.7-.0005V	0.	0.	40.	0.006	1748	10.8
4	.0001	.0005	0.7	0.	0.	40.	0.006	2246	13.3
5	.0001	.0005	0.3	0.	0.	40.	0.006	1086	6.0
6	.0001	.0005	0.3	0.	0.	40.	0.025	3520	18.6
7	.0001	.002	0.7-.0005V	0.	0.	40.	0.016	3306	21.4
8	.0001	.005	0.3	1.	100.	.01	0.025	68	1.4

The other data listed in the table are:

G the overall structural damping factor

W3 is the same as the MSC/NASTRAN parameter.

P0 the initial preload in the GAP elements (pounds/inch)

TF the final time for the integration process.

NS the number of integration time steps to reach TF

CPU the cpu time in sec to reach TF running on the Cray-YMP

In the first three cases the effect of the error tolerance was studied for the purpose of establishing a “good” default value. For these three cases the friction was a simple linear function of velocity. The effects of pressure and temperature on the friction coefficient was ignored. Clearly, one can see from Fig. 3 that varying the RTOL1 value from .00001 to .001 does not have a significant effect on the response of the chosen degree of freedom on the pad. Since one would expect a discrepancy between the three curves to increase with time, Fig. 4 zooms in on the last .001 seconds so that the differences can be seen more clearly.

Again, the differences are small. It is obvious that as the value of RTOL1 is increased, the number of integration steps, NS, required to reach TF, as well as the CPU time, is reduced. Clearly, if the requested error is too small, there will be an increase in the computation cost. Therefore, for all subsequent calculations the RTOL1 value was set to .0001 as a compromise between accuracy and cost. One can also readily see from Fig. 4 that all three cases exhibit squeal, because of a clear growth in the response.

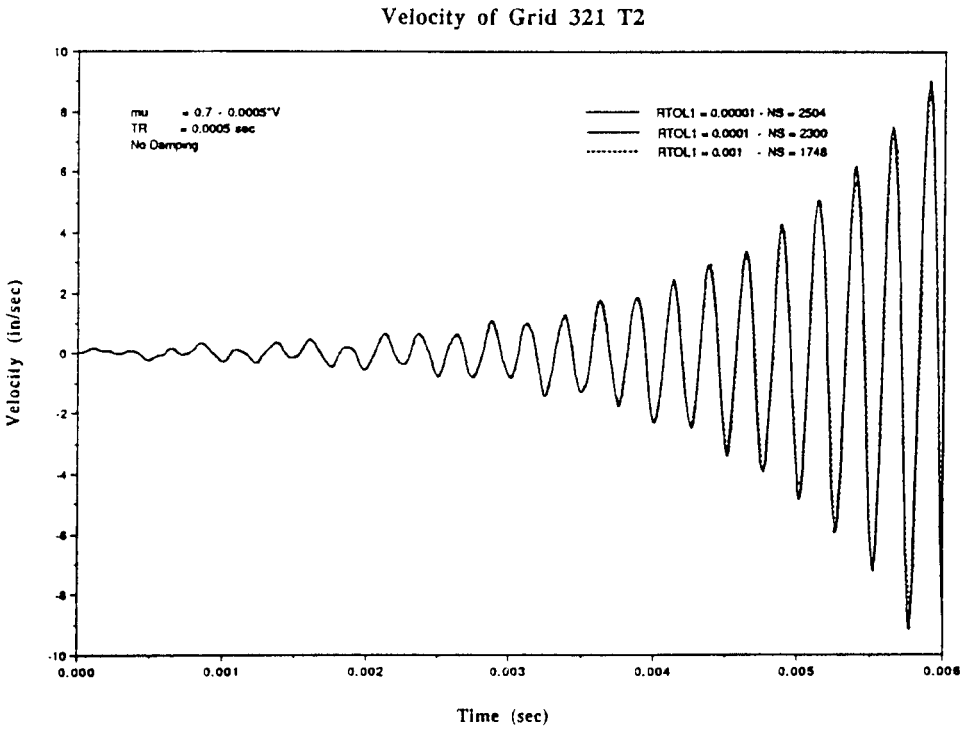

Fig. 3 Effect of RTOL1 on the solution accuracy

Figure 5 illustrates the comparison between Case 2 and 4 where the coefficient of friction is changed from a linear function of velocity to a constant value of 0.7. Note that the growth of the response is larger when μ is a function of velocity.

Figure 6 exhibits the difference of three cases, Cases 2, 4, and 5. This figure shows the effect of the μ on brake squeal. When μ has a constant value of 0.3 there is no squeal. This is an important fact because the same behavior is also readily seen in actual brakes.

Figure 7 shows the response for μ=0.3 only, with integration time extended from 0.006 sec to 0.025 sec. The time was increased to insure that squeal would not occur at some later time.

Lastly, Fig. 8 demonstrates the effect of the applied load rise time. When the rise time is short, Case 2 (0.0005 sec) squeal occurs quickly. When the rise time is longer, Case 1a (0.002 sec), it takes significantly longer for squeal to begin. From this result, one can conclude that there is no point in delaying the application of the applied brake load. Rather, the load should be applied as quickly as possible.

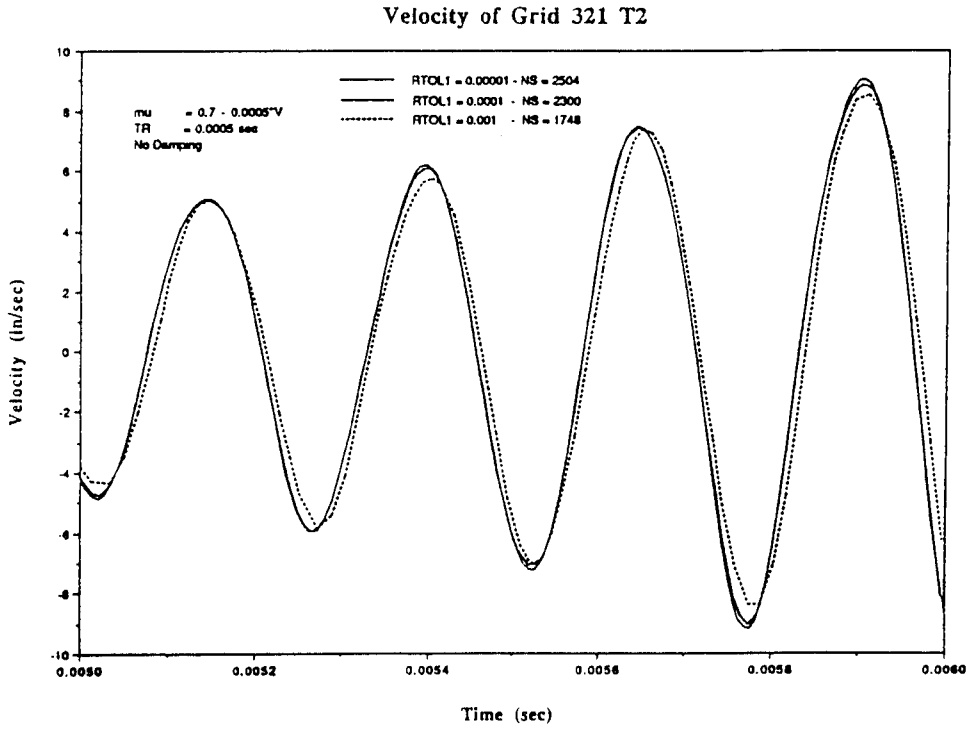

Fig. 4 Effect of RTOL1 on the solution accuracy (enlarged view)

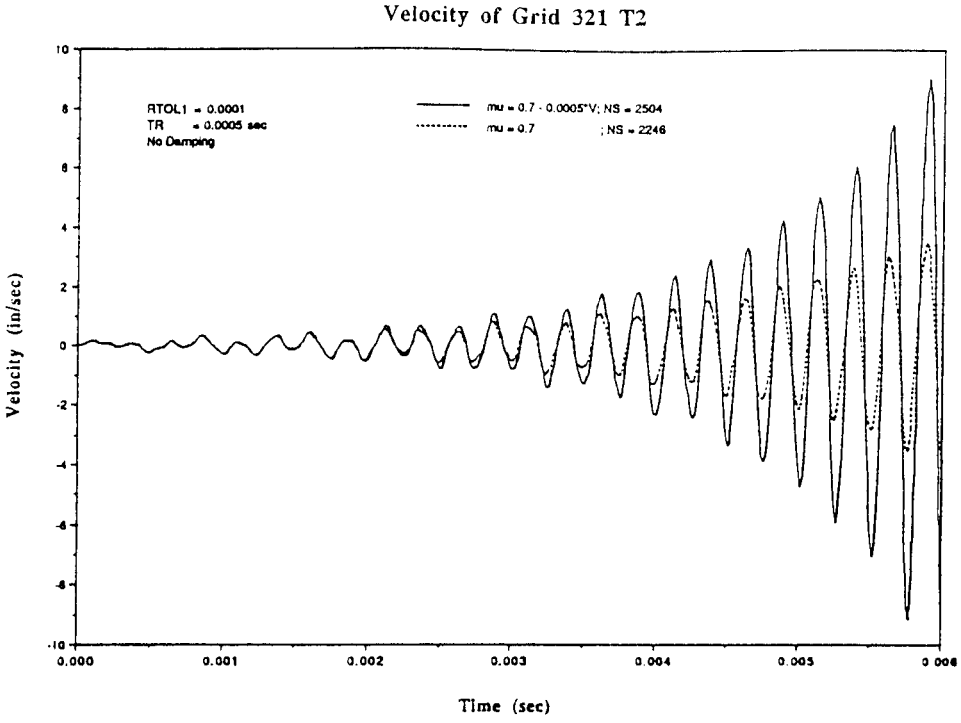

Fig. 5 Effect of μ variation wrt. velocity on brake squeal

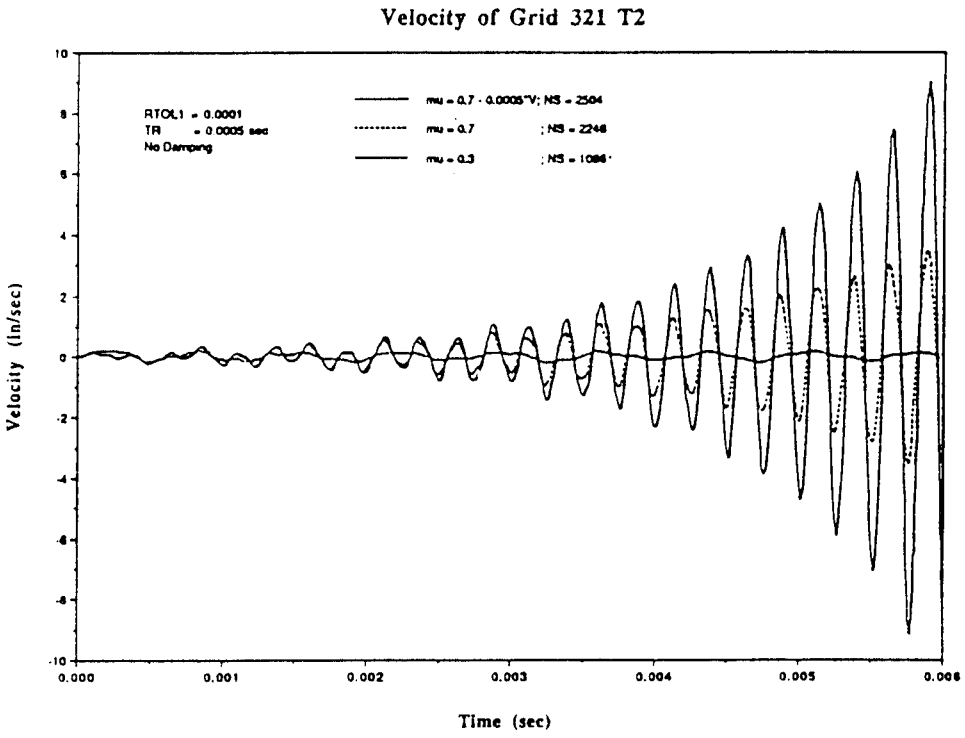

Fig. 6 Effect of μ variation on brake squeal

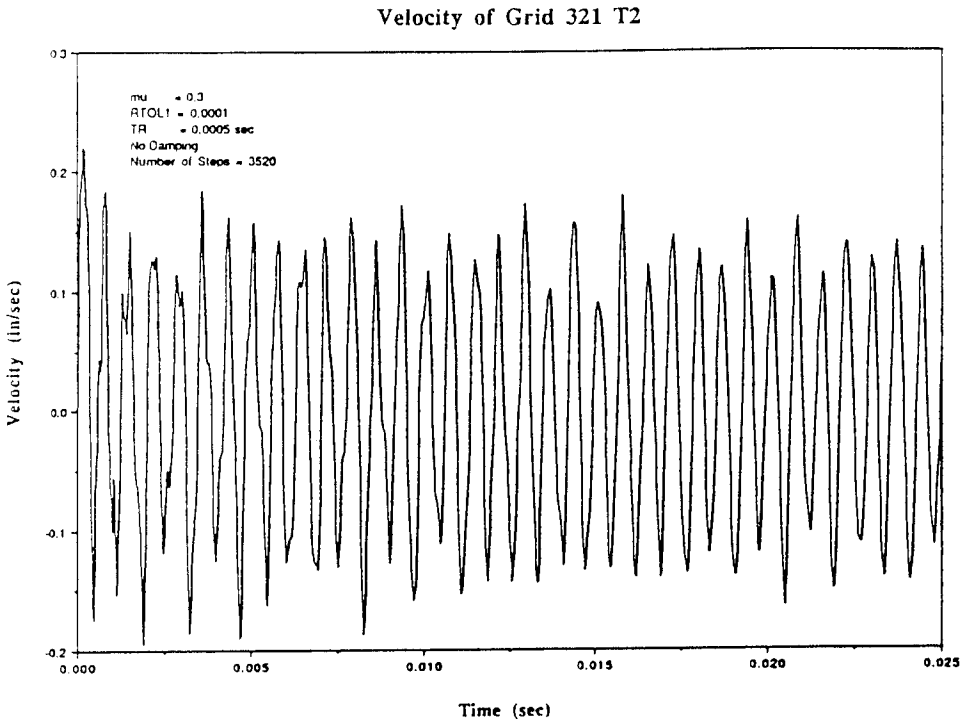

Fig. 7 Lack of squeal for μ=0.3

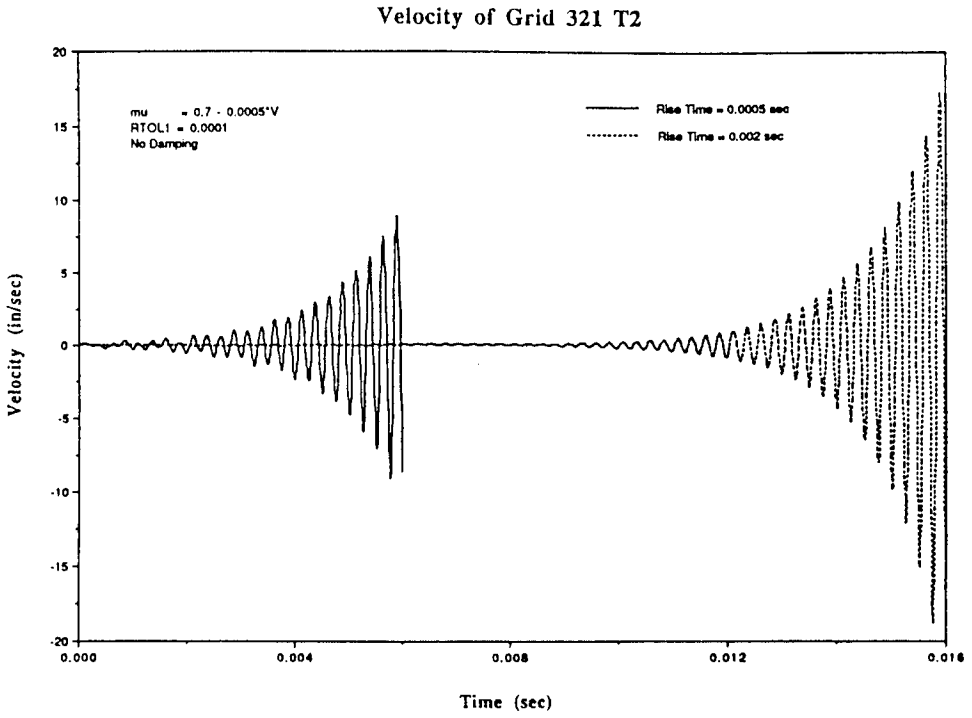

Fig. 8 Effect of load rise time on brake squeal

4.0 CONCLUSIONS

It was determined that many of the physical effects of brake squeal can be shown by simulation using sophisticated modeling and analysis. The example model exhibits many of the characteristics of the published experiments. Large order models using BSQL and similar codes were attempted and showed promise but suffered from a lack of good empirical friction data or from modelling mistakes. Finally the small changes due to variations in the integration error controls indicate that the divergence is due solely to the analytic model, and not caused by numerical problems.

REFERENCES:

1.Abrishaman, M., SDRC Friction Model, Proposal to GM, 1984.

2.Antonion, S.S., "The Friction Speed Relation form Stick Slip Data," Wear, Vol. 36, 1976.

3.Bowden, F.P., Tabor, D., **The Friction and Lubrication of Solids**, Oxford University Press, 1964.

4.Brown, P. N., Hindmarsh, C., and Petzold, L. R., “Using Krylov Methods in the Solution of Large-Scale Differential-Algebraic Systems,” University of Minnesota, Tech. Rep. TR 93-37, May 1993.

5.Busby, H.R., Lyons, W.M., Singh, R., "Stability Analysis of a Brake Squeal Model," Noise Conference, Ohio State University, June 1985.

6.Den Hartog, J.P., **Mechanical Vibrations**, McGraw-Hill, 1956.

7.Earles, S.W.E., Chambers, P.W., "Predicting Some Effects of Damping on the Occurrence of Disc Brake Squeal Noise," ASME Winter Meeting, Nov. 1985.

8.Etkin, B., **Aircraft Stability and Control**, Wiley, 1982.

9.Gu, J.C., Rice, J.R., et al, "Slip Motion and Stability of a Single Degree of Freedom Elastic System with Rate and State Dependent Friction," J. Mech. Phys. Solids, Vol. 32, No. 3, pp. 167-196, 1984.

10. Kato, S., "Some Considerations on Characteristics of Static Friction of Machine Tool Slideway," J. Lubr. Tech., Vol 94, pp. 234-247,1972.

11. Kragelskii, I.V., Dobychin, M.N., Kombalov, V.S., **Friction and Wear: Calculation Methods**, Pergamon Press, 1982.

12. Lyons, V.M., Busby, H.R., Singh, R., "Pin Disk Modeling Concept Applied to the Brake Squeal Problem," ASME Design Conference on Mechanical Vibration and Noise," Cincinnati, Ohio, Sept. 1985.

13. MacNeal, R.H., The Dynamics of Rotating Elastic Bodies, MSR-36, 1973.

14. Mohamed, M., "A Study on the Mechanics of Friction Noise," Ph.D. Thesis, Clarkson University, 1987.

15. Moon, F.C., **Chaotic Vibrations: An Introduction**, Wiley, 1987.

16. Muiakami, H., et al., "A Study Concerned with a Mechanism of Disc Brake Squeal," NISSAN Motor Co., 1983.

17. Oden, J.T., Martins, J.C., "Models and Computational Methods for Dynamic Friction Phenomena," Comp. Meth. Appl. Mech. Eng. Vol 52, pp. 527-634, 1985.

18. Park, K.C., Underwood, P.G., "A Variable Step Central Difference Method for Structural Dynamics," Comp. Meth. Appl. Mech. Eng., Vol 22, pp. 241-258, 1980.

19. Petzold, L. R., Ren, Y., and Maly, T., “Numerical Solution of Differential-Algebraic Equations with Ill-Conditioned Constraints,” University of Minnesota, Tech. Rep. TR 93-59, May 1993.

20. Rabinowicz, E., **Friction and Wear of Materials**, Wiley, 1965.

21. Rao, R.S., Rieger, N.F., "Brake Squeal Problem in Underground Trains," Reference 4, pg. 337, Sept. 1984.

22. Schwartz, H.W., Hays, W.D., Tarter, J.H., "Brake Noise Analysis: A Systematic Approach," Automotive Engineer, 1986.

23. Srinivasan, V., "Dynamic Friction, **Large Space Structures: Dynamics and Control**, Springer, 1988.

24. Timoshenko, S., Young, D.H., Weaver, W. **Vibration Problems in Engineering**, Wiley, 4th. ed., 1974.

25. Tolstoi, D.M., "Significance of the Normal Degree of Freedom and Natural Normal Vibrations in Constant Friction," Wear, Vol. 10, pp. 199-213, 1967.